Macroscopic and mesoscopic surface diffusion from a deposit formed by a Stranski-Krastanov type of growth: Pb on Cu(100) at above one layer of coverage

G. Prévot, C. Cohen, J.-M. Guigner, and D. Schmaus

Groupe de Physique des Solides, Universités Paris 7 et 6, UMR-CNRS 75-88, 2 place Jussieu, 75251 Paris Cedex, France

(Received 28 October 1999; revised manuscript received 29 December 1999)

Under ultrahigh-vacuum conditions, we have studied the diffusion from Pb deposits on Cu(100), at above one-layer coverage, in the 250–625 K temperature range. The growth mode is Stranski-Krastanov, and the deposits consist of thick three-dimensional Pb islands which form above a dense Pb single layer. This latter layer has a two-domain structure which ''melts'' around $T_M = 520$ K. In the 475–625 K temperature range, we have measured the spread of the deposits in the mm range, using *in situ* Rutherford backscattering analysis. To study diffusion at lower temperature, on a smaller scale, the Pb layer between the islands has been removed by sputtering around 150 K. We have then studied, in the 250–380 K temperature range, the kinetics of its reformation by using *in situ* Auger spectroscopy. In these experiments the Pb diffusion is followed over distances of the order of the spacing between Pb islands, i.e., about 1 μm. Our measurements demonstrate that the diffusing species is a Pb adatom moving above the dense Pb layer, leading to its spread with a quasiconstant Pb concentration, the adatom source being the Pb islands. We have analyzed our results via numerical integration of a diffusion equation with a concentration-dependent diffusion coefficient, using the finite-difference method. This analysis provides the activation energy E_T governing the process. E_T is the sum of two characteristic energies E_S and E_d. E_S is the formation energy of Pb adatoms from the islands, and E_d the activation energy for the motion of these adatoms on the Pb layer. E_d is markedly higher below T_M than above, indicating that when the Pb layer is structured, the diffusion is probably limited by the crossing of domain boundaries.

I. INTRODUCTION

In this paper we report on an experimental study of surface diffusion in a system with heterogeneous morphology resulting from a Stranski-Krastanov type of growth. The system chosen is Pb on Cu(100). When Pb is deposited at room temperature (RT) on Cu, it was observed long ago[1] that a continuous Pb single layer wets the substrate surface. If deposition is continued once this layer is formed, the additional Pb atoms agglomerate in three-dimensional (3D) islands, which cover a small fraction of the surface. When such a deposit is annealed, Ostwald ripening takes place: the concentration of 3D islands decreases, the larger islands growing at the expense of smaller ones.[2,3] This process has been extensively studied both theoretically[4] and experimentally on various systems.[5–9] Like the growth process, Ostwald ripening on a Stranski-Krastanov system is related to adatom diffusion on the top of a continuous layer which wets the substrate. In what follows, we shall adopt the notation proposed in Ref. 8. We thus call E_{d0} and E_d the activation energies associated, respectively, with the diffusion of adsorbate adatoms on the substrate surface plane and on the top of the wetting layer of adsorbate atoms. The sublimation energy of an adsorbate atom from a three-dimensional island of size i is called $L(i)$. $L(i)$ increases with i, which is the origin of Ostwald ripening. The adsorption energy of an isolated adsorbate adatom on top of the wetting layer is called E_a. Thus the formation energy of a Pb adatom on this layer, from an island of size i, is $E_S = L(i) - E_a$. For large island sizes, $L(i)$ tends asymptotically toward a constant value L_0, and E_S becomes constant. If the deposit has only been achieved on part of the substrate, its spread toward uncovered regions is then expected to depend on the energies E_S, E_d, and E_{d0}. Moreover, as a consequence of the interactions between adsorbate atoms, E_{d0} may vary markedly with coverage. The processes leading to the deposit spread are thus complex and, as a matter of fact, different behaviors have been observed for the spread of various types of deposits. In particular, the systems Ag/Si(111),[10–12] Ag/Ge(111),[13] Ag/Fe(110),[14] and Ag/Cu,(110)[15] which all correspond to a Stranski-Krastanov type of growth, have been studied in detail.

We have chosen to study the system Pb/Cu(100) for two main reasons. First, a great deal of information is available in the literature, not only on the crystallographic structure and the morphology of such deposits but also on Pb diffusion below one-layer coverage. Second, many characteristics of this system make it particularly well adapted for the study of the basic processes governing the diffusion at high coverage, i.e., in presence of Pb islands. Let us mention the fact that the wetting Pb film on which the islands form consists, as indicated above, of a single layer. Let us also underline that the melting temperature of the Cu substrate (1358 K) is much higher than that of bulk Pb (600 K), and than the temperature associated with the order-disorder transition of the wetting single Pb layer (around 500 K; see Sec. II). Such a feature makes a study of Pb diffusion in a wide temperature range possible, and allows one to search for the possible influence of the structural order of the Pb wetting layer.

II. Pb/CU(100) SYSTEM

A. Deposit structure and morphology

Pb and Cu both have a fcc structure but very different lattice parameters. They are practically immiscible in bulk

below the Pb melting temperature.[16] For the deposits, we define the coverage θ as the ratio between the areal density of Pb atoms and the density of sites on the (100) Cu face. In what follows we detail the characteristics of deposits formed at RT with different coverage.

The saturation coverage θ_S of the continuous single layer which forms before three-dimensional growth is $\theta_S = 0.6$.[17,18] Below a critical coverage $\theta_C = 0.25$, no Pb structure is observed by low-energy electron diffraction (LEED),[1] and scanning tunneling microscopy (STM) measurements demonstrate that Pb forms a disordered surface alloy.[19,20] Above θ_C, one observes successively a $c(4 \times 4)$ structure,[1] which is determined by STM to be a surface alloy,[19,20] a $c(2 \times 2)$ structure which corresponds to a pure Pb top layer,[1,21] and, finally, a pure Pb top layer with a $c(5\sqrt{2} \times \sqrt{2})R45°$ two-domain structure, which forms above a coverage θ_0 slightly lower than θ_S.[1,17,19,20,22] This latter structure will hereafter be called "$5\sqrt{2}$." For the three structures, temperatures characteristic of order-disorder transitions have been observed by thermal energy atom scattering, and associated with melting. The "melting" temperature T_M of the $5\sqrt{2}$ structure was measured to be 490 K.[23]

Above θ_S, 3D tabular islands with parallelepiped shapes form on the top of the $5\sqrt{2}$ structure. Their structure, morphology, and epitaxial relationship were studied in detail in Refs. 2 and 24. Their typical dimensions are 150 Å in height and, laterally, a few 1000 Å. The mean island density is typically 2.5 μm^{-2}, which corresponds to a mean distance of 0.6 μm between islands. The islands cover typically 10% of the deposit area. When such a deposit is annealed for about 1 h around 550 K, Ostwald ripening takes place. Deposits annealed in such a way have been analyzed *ex situ* using a scanning electron microscope.[24] The remaining islands are then of tabular triangular shape with, typically, 1000 Å in height and 1 μm in lateral dimensions. Their density is about 0.02 μm^{-2}, which corresponds to a mean distance between islands of several micrometers. They cover a negligible fraction of the deposit area.

B. Pb diffusion below T_M

Systematic measurements of Pb diffusion, below one-layer coverage, as a function of temperature (T) and coverage θ have been previously performed by Rutherford backscattering (RBS).[18] The analysis of the deposit spread for various annealing times provided the chemical diffusion coefficient $D(\theta, T)$. An overall increase of D with θ was observed (more than three orders of magnitude between low θ values and θ_S), showing strong repulsive Pb-Pb interactions in nearest-neighbor positions. However, a definite lowering of D is also shown in the (θ, T) domain where ordered Pb structures exist. This lowering is probably due to anticorrelation between consecutive Pb moves: a jump which locally affects the structural order is, most of the time, followed by a jump in the opposite direction which restores the order. The activation energy associated with jumps of isolated Pb atoms was determined to be 0.68 ± 0.02 eV.

III. EXPERIMENTAL PROCEDURES

A. Procedures

In the work presented here, our aim is to study diffusion, at a coverage $\theta > \theta_S$, over a wide temperature range. For realistic annealing times (between a few minutes and a few days), the corresponding spreads were of course very different. We have thus used two different analyzing techniques.

The first technique was adapted to the measurement of spreads in the mm range, corresponding to annealing temperatures between 470 and 625 K. For this purpose, we used the same procedure as in Ref. 18. A Pb disk, with a diameter dimension of a few mm, was deposited at RT at the center of the sample. At given annealing temperature, the Pb concentration profiles, along two perpendicular lines crossing at the deposit center, were determined in situ by RBS for various annealing times.

The second technique, used to study spreads in the μm range generated by annealing in the 250–375 K temperature range, is based on measurements by Auger electron spectroscopy (AES). In these experiments, the deposit, also achieved at RT, was sputtered at low T (around 150 K), with a sputtering ion dose sufficient to remove most of the wetting single layer of Pb, but low enough to leave on the sample most of the Pb atoms in the islands. The removal of the wetting layer was checked by AES, and the temperature was low enough to "freeze" this metastable configuration. The sample was then heated, at a fixed temperature between 250 and 375 K, allowing one to follow by AES the kinetics of reformation of the wetting layer between the islands. The spread was thus observed over distances of the order of the mean spacing between islands, that is, in the μm range. This spacing could be increased by, typically, one order of magnitude, through Ostwald ripening, by annealing around 550 K a deposit achieved at RT, prior to sputtering at low T. At each stage of the experimental procedure described above, the quantity of Pb on the surface was precisely determined by RBS.

A qualitative observation by AES of the reformation of the Pb wetting layer after sputtering was already reported in Ref. 25. In this work, very large islands were formed by annealing a thick Pb deposit at 583 K. Sputtering and AES measurements were then performed at this very same temperature; these latter measurements showed a very fast reformation of the Pb wetting layer.

B. Experimental setup

The experiments were performed in an ultrahigh-vacuum goniometric chamber (with a base pressure of 10^{-11} Torr) coupled to a 2.5-MV van de Graaff ion accelerator. The chamber was described in detail in Ref. 26. The sample, a Cu(100) crystal, is a disk mechanically and electrochemically polished. It is mounted on the goniometer. Its thickness is 4 mm and its diameter dimension is 12 mm. The sample holder is a furnace and the sample can be heated from the backside up to 1100 K. It can also be cooled down to 120 K by connecting it to a cold point at liquid-nitrogen temperature. The temperature is measured by a thermocouple set in a hole made in the sample side. After Ar sputtering at RT and annealing at 800 K, a Pb deposit is achieved by evaporation on the sample at room temperature. Diaphragms can be placed in front of the sample, very close to it, in order to define the deposit geometry. This geometry was chosen to be a disk with a diameter dimension of 2.5 mm located at the center of the sample. AES and LEED measurements were performed *in situ* using a four-grid LEED-Auger system with

an electron gun perpendicular to the sample surface. The electron spot size is between 0.5- and 1-mm diameter.

To obtain accurate Pb concentration profiles by RBS measurements, the direction and the impact position of the incident beam (^{4}He$^+$ ions for the experiments reported here) were fixed by a set of diaphragms. The backscattered ions are counted and analyzed in energy using a collimated bakeable surface barrier silicon detector set at a detection angle of 135°. Integration of the Pb signal in a RBS spectrum provides the absolute amount of Pb atoms per unit area, averaged over the beam impact on the sample. Calibration is obtained using a reference standard containing an amount of Bi, implanted in preamorphized Si, known with a precision of 2%.[27]

In order to measure concentration profiles, the sample is translated in front of the beam with an accuracy better than 0.1 mm, successively along two perpendicular lines x and y which cross at the deposit center. The initial profile, after deposition, was systematically measured. The coverage was found to be uniform within less than 5%. Thermal desorption due to annealing was always found to be negligible in the experiments reported here. During all the experiments, we never observed any detectable Pb loss induced by the probing beam. The beam intensity profile is measured along the x and y directions before each experiment. For this purpose, backscattering scans are performed by moving successively across the beam spot two perpendicular wires of tungsten, 0.1 mm thick. In both directions, we found nearly Gaussian profiles with a full width at half maximum of 0.4–0.5 mm.

IV. DATA REDUCTION

A. RBS spectra

Two typical RBS spectra are presented in Fig. 1(a). They were obtained with a ''random'' orientation of the probing beam (away from any major crystallographic direction of the substrate) on the central part of a deposit achieved at RT, and corresponding to $\theta = 5.6 \, \theta_S$. The first spectrum was recorded just after deposition, and the second one after 10 min annealing at 593 K. The Pb signal in the first spectrum is a narrow peak. The energy loss of the incoming and outcoming ions which cross the Pb islands (which are about 150 Å thick) is of the order of magnitude of the depth resolution associated to the energy resolution of the detector. The Pb signal in the second spectrum is much broader, revealing the presence of much thicker islands (about 1000 Å thick) formed by Ostwald ripening during annealing. The lower-energy part of the Pb signal on such a spectrum is affected by the presence of a background originating from signal pileup in the electronics. To minimize this background, we decided to record channeled spectra, the incoming beam being aligned with the [001] axis of the Cu crystal, perpendicular to the sample surface. Figure 1(b) shows two spectra collected in this geometry on the deposits which were also studied in random geometry [Fig. 1(a)]. The backscattering rate on Cu atoms is 30 times lower than for a random orientation of the incoming beam. As the background contribution below the Pb peak is proportional to this rate, the gain in sensitivity and in counting time is spectacular. With such a channeling geometry, we were able to determine Pb amounts of 10^{13} at/cm^2 (i.e., about 10^{-2} single layer) within 2 min
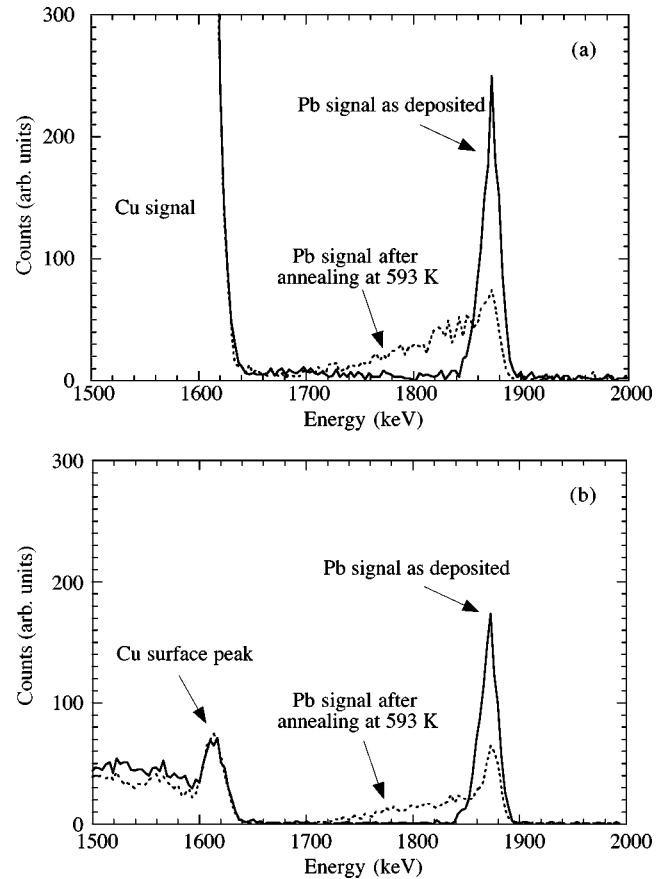
FIG. 1. RBS spectra obtained with a 2 MeV ^{4}He$^+$ beam on a Pb deposit achieved at RT. Pb coverage: $\theta = 5.6 \, \theta_S$; detection angle: 135°. Full lines: spectra registered before annealing. Dotted lines: spectra registered after 10 min annealing at 593 K. The four spectra were obtained with the same number of incident ions. (a) Random spectra. (b) Channeled spectra (note the very low background below the Pb signal).

with statistical uncertainties of the order of 3%. The small remaining background contribution was systematically determined and subtracted by collecting spectra on uncovered parts of the sample.

When attempting to determine the absolute Pb coverage from channeled spectra collected on regions of the deposit which contain 3D Pb islands, one has to account for the channeling effects inside these islands which also lower the backscattering rate from Pb atoms. For this purpose, a few spectra were obtained with low beam currents in random geometry. Their comparison with the corresponding channeled spectra provided the ratio χ of the channeled to random backscattering yield in the islands. The value of χ, which reflects the crystalline quality of the islands, depends markedly on the annealing temperature T_A. However, at a given T_A, all over the regions of the deposit which contain islands, χ reaches a constant value after a time much shorter than the one after which the deposit spreads over distances in the mm range. Quite surprisingly, χ does not vary uniformly with T_A. It first decreases markedly, from $\chi = 0.60$, on unannealed deposits made at RT, to $\chi = 0.30$ for $T_A = 475$ K. For higher T_A, χ increases. For instance, at $T_A = 595$ K, just below the melting temperature T_B of bulk Pb ($T_B = 600$ K), we found $\chi = 0.50$. After annealing just above
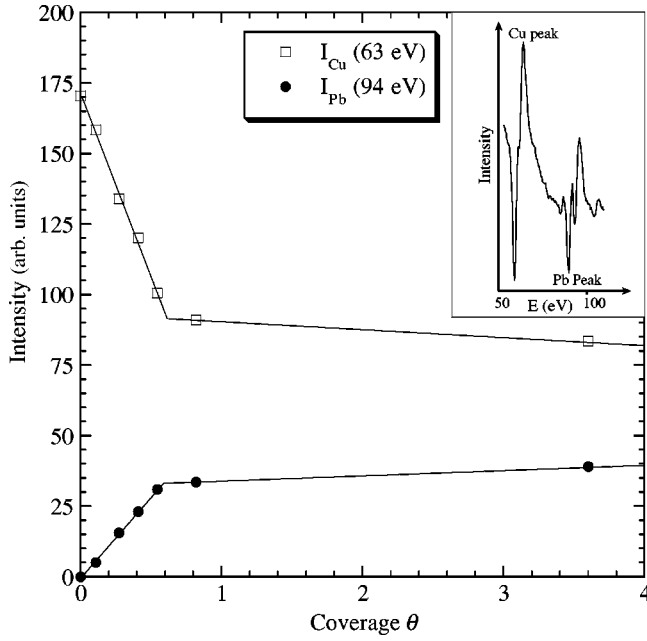
FIG. 2. Variation of the Cu and Pb AES signals with Pb coverage θ during Pb deposition at RT. The calibration of the coverage θ was achieved by RBS.

T_B, at 625 K, we measured $\chi = 0.75$. All the values of χ reported here correspond to measurements at RT, after annealing.

B. AES results

In Fig. 2 we show the evolution of the Cu and Pb AES signals, of respective intensities I_{Cu} and I_{Pb}, during Pb deposition at RT. A typical AES spectrum is also shown in the inset. The behavior of I_{Cu} and I_{Pb} with θ is characteristic of the Stranski-Krastanov growth mode, with a wetting film restricted to a single layer. The values of θ represented on the figure have been calibrated by RBS. We shall call I^0_{Cu} and I^0_{Pb} the AES signals corresponding, respectively, to pure bulk Cu and Pb. We shall also assume a linear variation of the signals I_{Cu} and I_{Pb} as long as Pb wets the Cu substrate ($\theta < \theta_S$). Then the variation of the AES signals in Fig. 2 can be adjusted by

$$I_{Cu} = I^0_{Cu} - a\,\theta/\theta_S$$
$$I_{Pb} = b\,\theta/\theta_S \qquad \text{for } \theta \lesssim \theta_S$$

and $\qquad\qquad\qquad\qquad\qquad\qquad\qquad\qquad$ (1)

$$I_{Cu} = (I^0_{Cu} - a)(1 - \alpha_{IS})$$
$$I_{Pb} = b(1 - \alpha_{IS}) + I^0_{Pb}\alpha_{IS} \quad \text{for } \theta > \theta_S$$

In relation (1) we call α_{IS} the fraction of the deposit area which is covered by Pb islands ($\alpha_{IS} = 0$ when $\theta \lesssim \theta_S$). When adjusting the experimental results of Fig. 2, we obtained $\alpha_{IS} = 0.09$ for $\theta = 5.6\,\theta_S$, in very good agreement with RBS, STM, and atomic force microscopy measurements.[2,24] The evolution of the Cu and Pb signals above θ_S demonstrate that $\alpha_{IS}(\theta)$ increases slowly with θ above θ_S.

We have followed by AES the kinetics of reformation of the wetting Pb layer between the islands at given T, after its
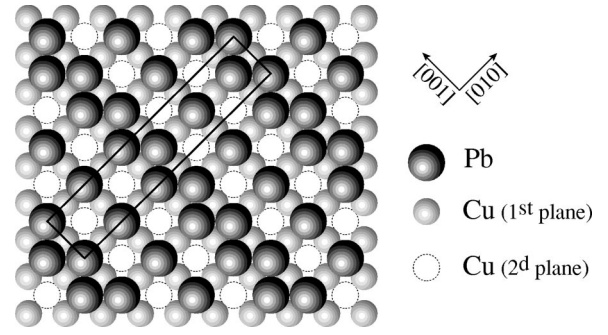
FIG. 3. Schematic representation of one domain of the $5\sqrt{2}$ structure formed by Pb atoms on a Cu(100) surface.

removal by sputtering at low T. This reformation takes place at the expense of the Pb islands, and thus changes both their mean height h (expressed in number of layers) and the fraction α_{IS}. Two extreme assumptions consist in considering that either h or α_{IS} remains constant. We have verified that choosing one or the other hypothesis does not lead to significant modifications in what concerns the conclusions of the data reduction. For instance, assuming h to be constant, and calling $\theta_S\alpha_{ML}$ the mean Pb coverage between the islands, one obtains

$$I_{Cu} = (1 - \alpha_{IS})(I^0_{Cu} - a\alpha_{ML}) \qquad (2)$$

and

$$I_{Pb} = \alpha_{IS}I^0_{Pb} + (1 - \alpha_{IS})b\alpha_{ML}, \qquad (3)$$

The measurement of I_{Cu} and I_{Pb} thus provide both α_{IS} and the mean Pb coverage $\theta_S\alpha_{ML}$ between the islands, which is the quantity to be determined in order to follow the reformation of the wetting Pb layer.

V. RESULTS AND INTERPRETATION

A. Macroscopic Pb diffusion in the 475−625 K temperature range

As indicated in Sec. III A, in that temperature domain, for the annealing times considered here, the spread, in the mm range, is followed by RBS measurements. However, in conjunction with the determination of the Pb coverage profile by RBS, the deposits were systematically studied by LEED.

1. Analysis of the deposits by LEED

a. Before annealing. After Pb depositions with coverage close to $\theta = 6\theta_S$, the LEED diagram at RT corresponds to a well-organized $5\sqrt{2}$ structure, characteristic of the Pb wetting layer (see Fig. 3). However, in the present experiments, the intensities of the spots corresponding to each of the two types of domains of this structure were very different, demonstrating that one orientation is by far dominant. This asymmetry was systematically observed on all the deposits achieved, and the preferred domain orientation was always the same. This behavior is probably related to a small miscut of the Cu crystal surface with respect to the (100) direction. As can be seen in Fig. 3, the $5\sqrt{2}$ structure consists of a succession of $c(2\times2)$ stripes and antiphase boundaries, along either the [001] or [010] directions, depending on the
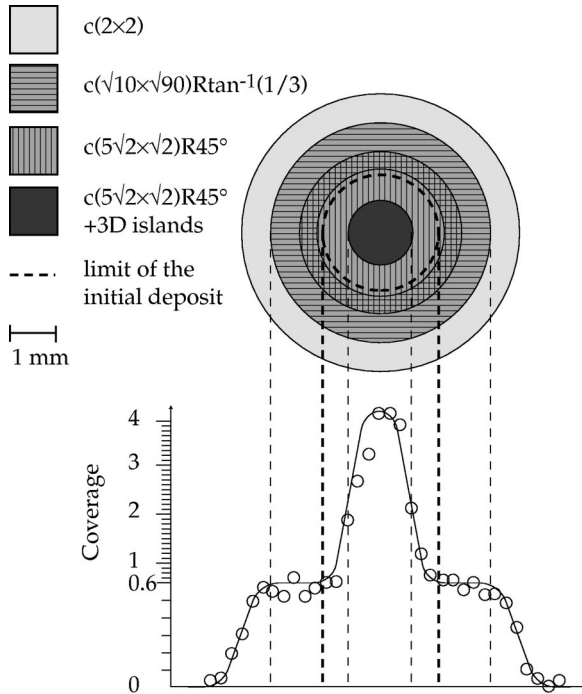
FIG. 4. Structures observed by LEED on the various regions of a Pb deposit annealed for 90 min at 533 K, and a concentration profile obtained by RBS (note the change in the vertical scale).

type of domain, and the ''open'' direction for adatom diffusion is obviously along the stripes. As one domain orientation is favored, we could then expect some asymmetry in the deposit spreads. To check this possibility with an optimal accuracy, the x and y directions chosen for measuring the Pb coverage profiles were the [001] and [010] directions, respectively.

We observed by LEED that spots corresponding to the $5\sqrt{2}$ structure disappear abruptly at 523 K. This change is reversible with T, with very weak hysteresis. We have indicated in Sec. II that the ''melting'' temperature of the $5\sqrt{2}$ structure was measured to be $T_M = 490$ K in Ref. 23, i.e., 33 K lower than what we observe. We believe that this systematic discrepancy is mostly due to differences in the ways the sample temperature is measured. For the sake of consistency with our measurements of deposit spreads as a function of T, in what follows we will set $T_M = 523$ K.

b. After annealing. In Fig. 4 we show a typical Pb coverage profile measured by RBS along the [001] direction after annealing for 90 min at 533 K a deposit with an initial coverage $\theta = 7\,\theta_S = 4.2$. In this figure we also show the structures shown by LEED observations at RT on the different regions which characterize this profile. Starting at the deposit center and going toward more and more peripheral regions, one observes, successively the following.

(i) A $5\sqrt{2}$ structure, with one preferred orientation, in the region of high coverage, i.e. in the presence of 3D Pb islands.

(ii) A $5\sqrt{2}$ structure, with one preferred orientation, in the most central part of the region with constant coverage $\theta = \theta_S = 0.6$.

(iii) A mixture of two different structures in the middle part of the region with constant mean coverage $\theta = \theta_S$. One is again the $5\sqrt{2}$ structure, with one preferred orientation. As
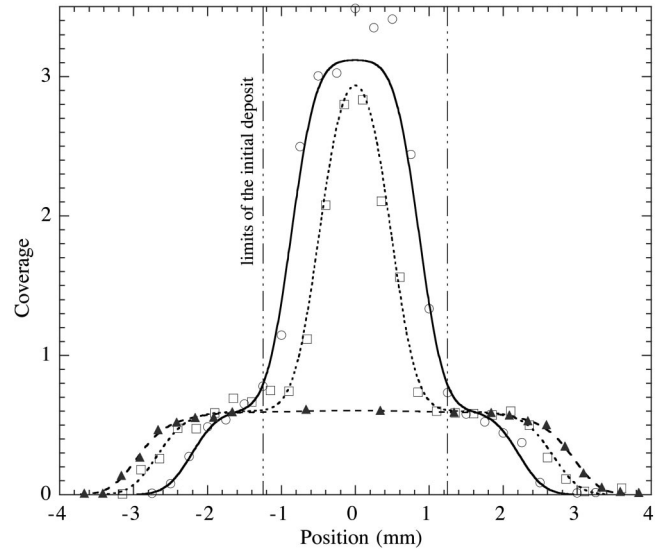
FIG. 5. Pb coverage profiles measured after various annealing times t on a deposit with initial uniform coverage $\theta_{in} = 3.2$ $= 5.3\ \theta_S$. Circles: $t = 10$ min; squares: 26 min; triangles: 42 min. All the lines are theoretical profiles corresponding to a value of the product $D_{ML}\epsilon$ equal to 8.10^{-6} cm^2 s^{-1} (see the text). The adjustment to this value has been obtained by fitting only the broadest profile corresponding to the time $t_c = 42$ min, at which the central zone with $\theta > \theta_S$ disappears.

this structure is characterized by a coverage θ_S, the second one also necessarily corresponds to a coverage close to θ_S (the uncertainty of our RBS measurements does not exceed $\Delta\theta = 0.02$). The interpretation of the LEED diagram led us to the identification of a $c(\sqrt{10} \times \sqrt{90})R\tan^{-1}(1/3)$ four-domain structure that will hereafter be called ''$\sqrt{10}$.'' Details on this ''new'' structure will be provided in a forthcoming paper. We have studied the evolution of its associated LEED diagram when increasing T. No sharp modifications are observed. The disorder increases continuously and strongly between RT and 330 K. In the entire temperature range in which this structure can be observed, we have not noticed a preferential orientation along one or another of its four domains.

(iv) A $\sqrt{10}$ structure alone on the external part of the region with constant coverage very near θ_S.

(v) A $c(2\times2)$ structure in the most peripheral region where the coverage θ decreases rapidly.

(vi) A 1×1 structure associated with the Cu(100) bare substrate in the region where no Pb was detected by RBS.

We never observed regions with a $c(4\times4)$ structure at the very edge of the Pb profiles. This is probably due to the fact that such regions have a very narrow spatial extension.

2. Pb diffusion and deposit spread above T_M

Above T_M, the spreading of the deposit was always observed to be isotropic. In Fig. 5 we present coverage profiles measured after annealing at 593 K for different duration. The initial profile has sharp edges and corresponds to a uniform coverage $\theta_{in} = 5.3\ \theta_S$. The observation of the profiles shown in Fig. 5 calls for several remarks.

(i) When the annealing time t increases, the width of the central zone, with $\theta > \theta_S$, i.e., containing 3D Pb islands, de-

creases, while its coverage remains equal to θ_{in} until the time t_c at which no more Pb islands are present. This observation implies that the deposit spread takes place at the only expense of the edges of the central zone. We have determined t_c from the time evolution of the Pb coverage at the center of the deposit. For instance, in the experiment illustrated in Fig. 5, we found $t_c = 42$ min.

(ii) Until t_c, the coverage profile outside of the central zone consists mainly of a plateau with constant coverage equal to θ_S. The width of this plateau increases with t.

(iii) The edges at the outer parts of respectively the central zone, with coverage θ_{in}, and of the plateau, with coverage θ_S, are steep.

Observations (ii) and (iii) demonstrate that there is an abrupt increase of the spreading velocity with θ around θ_S, i.e., when a dense wetting layer is completed. Thus the completion permits a new diffusion mechanism, much more efficient than the diffusion of Pb atoms on the Cu substrate which was studied in detail in Ref. 18. The most likely hypothesis is that this new mechanism is the diffusion of Pb adatoms on top of the dense wetting layer. Taking into account the experimental facts, we have attempted to fit the results through the integration of a diffusion equation with the following assumptions.

(a) The diffusion equation can be expressed in polar geometry as a function of a unique spatial coordinate, which is the distance r from the deposit center.

(b) The surface diffusion coefficient is constant in the central region of the deposit in which Pb islands are present. We call it D_{ML}. In this region, we have assumed that the Pb islands are in thermodynamic equilibrium with a constant coverage $\epsilon \theta_S$ of Pb adatoms on the top of the wetting layer. We have neglected any island nucleation during the deposit spread.

(c) D_{ML} is the diffusion coefficient for $\theta > \theta_s$; its value is significantly higher than the upper limit $D(\theta_S)$ corresponding to the coverage-dependent diffusion coefficients $D(\theta)$ for $\theta < \theta_S$. The values of $D(\theta)$ for $\theta < \theta_S$ were taken from Ref. 18.

(d) During annealing, and until its disappearance, the central region, which contains Pb islands, has a constant Pb coverage θ_{in}. For a given deposit spread, corresponding to a given annealing time, the area of this region is thus readily obtained from the conservation of the overall Pb amount.

With these assumptions, we have integrated numerically, using the finite-difference method, the diffusion equation

$$\frac{\partial \theta}{\partial t} = \frac{1}{r} \frac{\partial}{\partial r}\left(r D(\theta) \frac{\partial \theta}{\partial r}\right). \tag{4}$$

The profiles obtained by numerical integration were convoluted by the measured probing beam spot profile and compared to the experimental profiles. Two parameters are available in order to fit the measurements: D_{ML} and ϵ. In fact, as far as $D_{ML} \gg D(\theta_S)$, it appears that, for reasonable values of ϵ, ($\epsilon \ll 1$), the quality of the fits depends only on the value of the product $D_{ML}\epsilon$. This observation is not surprising, and can be associated with analytical predictions corresponding to a similar but simpler situation. Let us consider an initial one-dimensional profile $\theta(x) = \theta_S(1 + \epsilon)$ for $x \leq 0$ and $\theta(x) = 0$ for $x > 0$, with a diffusion coefficient $D(\theta) = D = \text{const}$

for $\theta \geq 1$ and $D(\theta) = 0$ for $\theta < 1$. In this case, one finds[28] that the position of the profile edge at time t depends indeed only on the product $D\epsilon$. This position is given by

$$x^2(t) = \frac{4D\epsilon t}{\sqrt{\pi}}. \tag{5}$$

In our more complex situation, the fact that the product $D_{ML}\epsilon$ remains a unique fitting parameter demonstrates that Pb diffusion on the Pb wetting layer is, by far, dominant with respect to Pb diffusion on the Cu substrate. This feature can be estimated in a quantitative way by comparing the fitting value of the product $D_{ML}\epsilon$ to the mean value: $D_{mean} = (1/\theta_S)\int_0^{\theta_S} D(\theta)d\theta$, which characterizes the diffusion on the Cu substrate. For all the calculated profiles that fitted our results, $D_{ML}\epsilon$ was higher than D_{mean} by an order of magnitude. Typical adjustments of the experimental results, providing the product $D_{ML}\epsilon$, are shown in Fig. 5, which corresponds to various annealing times at $T = 593$ K. The agreement is very good. All the calculated profiles represented were obtained using the value of the product $D_{ML}\epsilon$ that was determined when fitting the broadest profile, corresponding to the time $t_c = 42$ min.

The temperature dependence of the product $D_{ML}\epsilon$ for annealing temperatures higher than T_M (between 525 and 625 K) is very well described by an Arrhenius law with associated energy $E_T = 0.5 \pm 0.05$ eV. E_T is the sum of two energies associated with D_{ML} and ϵ, respectively. The first is the activation energy E_d corresponding to the diffusion of Pb adatoms on the wetting Pb layer. The second is the formation energy $E_S = L_0 - E_a$ of these adatoms from the Pb islands. One can see that the value of $E_T = L_0 - E_a + E_d$ is significantly smaller than the activation energy $E_{d0} = 0.68$ eV determined in Ref. 18 for the motion of isolated Pb atoms on the (100) Cu surface. Then, of course, E_d is markedly smaller than E_{d0}. The preexponential factor associated with the Arrhenius law which fits the temperature dependence of $D_{ML}\epsilon$ is the product of the prefactors associated with ϵ and with D_{ML}. The first one is nearly equal to unity[8]; the second can be considered as the product of an attempt frequency by the square of an elementary jump length. When taking for the attempt frequency a reasonable value of about 10^{13} Hz, we find a jump length of atomic size. Thus the diffusion of Pb adatoms on the wetting Pb layer above its melting temperature T_M is controlled by the activation energy associated with jumps between near neighbor sites.

3. Pb diffusion and deposit spread below T_M

In Fig. 6 we show a comparison of two concentration profiles, measured along the [001] and [010] directions, respectively, on a deposit with an initial coverage $\theta = 6.3\theta_S$, after annealing during 19.5 h at $T = 475$ K (i.e., below $T_M = 523$ K). The deposit spread is markedly larger along the [001] direction. This behavior may appear surprising on the isotropic (100) Cu surface. To account for the anisotropy of the deposits spread, we took benefit of the LEED observations discussed Sec. V A 1 b. These observations show that the only asymmetry between the [001] and [010] directions arises from the $5\sqrt{2}$ structure, in connection with the unequal proportion of each type of domain. The origin of the asymmetric spread must then be a very anisotropic diffusion in
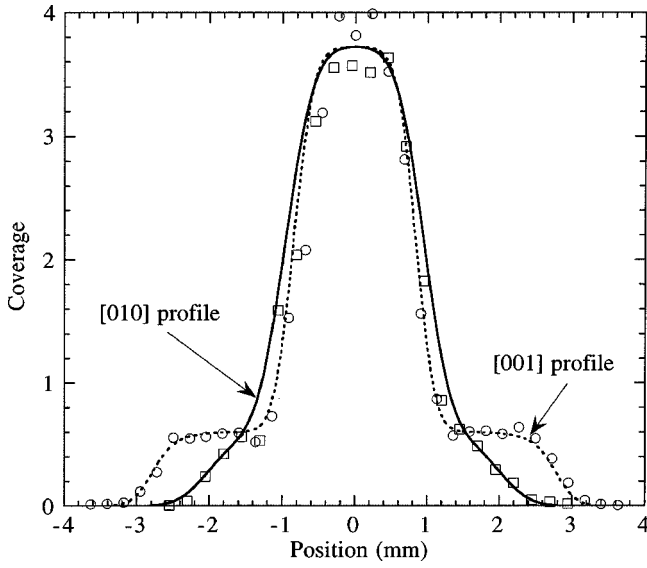
FIG. 6. Pb coverage profiles measured along the [001] (circles) and [010] (squares) directions on a deposit, with initial coverage $\theta = 3.8 = 6.3 \ \theta_S$, annealed at 475 K during 19.5 h. The best fits of the two profiles are represented by lines.

regions of the deposits where the $5\sqrt{2}$ structure is present. It is reasonable to assume that, on each of the two domains of the $5\sqrt{2}$ structure, diffusion takes place preferentially along the direction of the $c(2\times2)$ stripes. As one domain orientation is favored, most of these stripes are oriented along the [001] direction. This would explain the observed anisotropy of the spread.

To interpret the results we then had to introduce two coverage-dependent diffusion coefficients D_x and D_y, associated with the [010] and [001] directions, respectively. The diffusion equation in Cartesian coordinates is thus

$$\frac{\partial \theta}{\partial t} = \frac{\partial}{\partial x}\left(D_x(\theta) \frac{\partial \theta}{\partial x} \right) + \frac{\partial}{\partial y}\left(D_y(\theta) \frac{\partial \theta}{\partial y} \right). \qquad (6)$$

It has been discretized and integrated numerically as in Sec. V A 2.

In what concerns the coverage dependence of D_y, we made the same assumptions as for D above T_M. Below θ_S, we took the values $D(\theta)$ measured in Ref. 18. Above θ_S, D_y was assumed to be independent of θ ($D_y = D_{ML}$). The value of the product $D_{ML}\epsilon$ was deduced from the fit of the measured Pb spreads along the [001] direction, and found to be significantly greater than the value D_{mean} which characterizes the diffusion on the Cu substrate.

The spreading anisotropy could be well reproduced by considering that the diffusion along the x ([010]) direction was fully blocked in regions where the $5\sqrt{2}$ structure was present. We know (see Sec. II) that the $5\sqrt{2}$ structure forms above a coverage θ_0 slightly lower than θ_S. Thus we have fixed an arbitrarily small value of D_x [at the scale of $D(\theta_0)$] in regions where the coverage exceeded the critical value θ_0. Below θ_0, we took $D_x = D_y = D(\theta)$. The value of θ_0 was determined by adjusting the calculated and measured profiles in the [010] direction.

In Fig. 7 we report on the values of the product $D_{ML}\epsilon$ obtained from the fits of the experiments performed at five
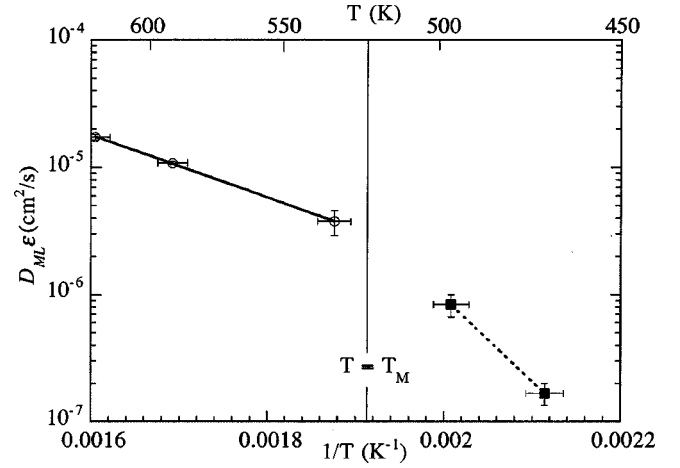
FIG. 7. Arrhenius plot corresponding to the temperature dependence of the product $D_{ML}\epsilon$ in the 425–625 K temperature range, i.e., below and above T_M. Above T_M, the values of $D_{ML}\epsilon$ concern both the [001] and [010] directions; below they are only related to diffusion along the [001] direction.

temperatures between 475 and 625 K. In the Arrhenius representation shown in Fig. 7, it appears clearly that the slope of the line joining the points corresponding to measurements at various T is markedly higher below T_M. The Arrhenius law corresponding to the two measurements below T_M has an associated energy E_T of 1 eV, i.e., twice the value found for measurements above T_M. In the meantime, no obvious discontinuity is observed around T_M in what concerns the value of the product $D_{ML}\epsilon$. The sudden increase of E_T around T_M is thus necessarily compensated for by a strong concomitant increase of the preexponential factor of the Arrhenius law. As a matter of fact, we find that the preexponential factor is about five orders of magnitude higher below T_M than above. Considering again realistic attempt frequencies around 10^{13} Hz, we deduce that the mean elementary jump length below T_M is a few thousand Å.

To attempt an interpretation of these spectacular and surprising results, we considered the fact that below T_M the Pb wetting layer is constituted by ordered domains. A reasonable value of the linear size of an individual domain in the $5\sqrt{2}$ structure is of the order of 1000 Å. With this in mind, our interpretation is that, below T_M, the limiting factor for Pb adatom diffusion on the wetting layer is the crossing of domain boundaries. We have already underlined that the sites available for Pb adatoms above the $5\sqrt{2}$ structure are on top of the $c(2\times2)$ stripes, and thus that the adatoms diffuse along these stripes. When an adatom meets a domain boundary it has no easy way to reach a $c(2\times2)$ stripe of the new domain. This may be the origin of the difficult domain boundary crossing. The mean elementary jump length is thus associated with the mean linear size of a domain. Let us call ΔE_T the difference between the values of E_T below and above T_M ($\Delta E_T = 1 - 0.5 = 0.5$ eV). In the frame of our interpretation, ΔE_T is equal to the difference ΔE_d between the activation energy for crossing domain boundaries below T_M and the one associated with atomic size jumps on the melted layer above T_M. The value of the activation energy for boundary crossing lies thus between 0.5 and 1 eV.

B. Mesoscopic Pb diffusion in the 250−380 K temperature range

As indicated in Sec. III A, in this temperature domain the spread, in the μm range, is followed by AES measurements. However, we have also performed some preliminary LEED observations. During sputtering, the wetting layer is removed. As the 3D islands occupy a minor fraction of the deposit area, the LEED diagram observed corresponds to the (100) Cu surface, as long as the sample is maintained at sufficiently low T. When the sample temperature is raised, in order to allow the reformation of the Pb wetting layer, the LEED diagrams observed show that, since the very beginning of the reformation, the ordered $5\sqrt{2}$ structure (and only this one) exists. This observation demonstrates that a dense ordered wetting layer with a coverage very close to θ_S begins to grow at the islands periphery. Such behavior again indicates that diffusion is much easier on the Pb wetting layer than on the (100) Cu substrate surface.

1. Pb diffusion from Pb islands previously annealed at 530 K

In these experiments, a Pb deposit, with an initial coverage $\theta = 7\theta_S$, was achieved on the whole sample surface. This deposit was then annealed for 1 h at 530 K, leading to a decrease of the island density due to Ostwald ripening. Thus, 3D Pb islands form with a size and concentration very close to those corresponding to the experiments performed between 475 and 625 K described above.

After sputtering at 150 K, the remaining coverage, measured by RBS, was found to be $\theta = 5\theta_S$. No detectable Pb signal could be observed on an AES spectrum. This feature demonstrates that the remaining Pb atoms are mostly all in 3D islands, which occupy a negligible fraction of the sample surface. The sample temperature was very rapidly raised up to 343 K. At this temperature, we have then followed by AES the evolution with time of the mean Pb coverage $\theta_S \alpha_{ML}$ between the islands (see Sec. IV). In fact, the LEED observations, discussed in the introduction of this section, demonstrate that α_{ML} can be identified to the fraction of the sample surface that is again covered by the dense $5\sqrt{2}$ structure.

The function $\alpha_{ML}(t)$ that was extracted from the AES measurements is shown in Fig. 8. To interpret this result, we compared it to a simulation of the time evolution of the surface coverage between the islands. This simulation was based, as in Sec. V A 3, on the numerical resolution of a two-dimensional diffusion equation, using the finite-difference method with diffusion coefficients depending on the coverage θ. In the simulations, the sample surface is a square with periodic boundary conditions. At time $t = 0$ it is only covered by 3D Pb islands, whose size and spatial distribution reproduce exactly an image obtained by scanning electron microscopy (SEM) on a very similar deposit that was also annealed at 530 K. As seen in Fig. 9, in the simulation the wetting layer reforms by coalescence of compact zones of quasi-isotropic slope, with a uniform coverage θ_S, which develop around the islands. This behavior is related to two assumptions that we were led to make in order to describe the experimental results properly, and that will be discussed below. The best adjustment by simulation of the function $\alpha_{ML}(t)$ extracted from our AES measurements is also
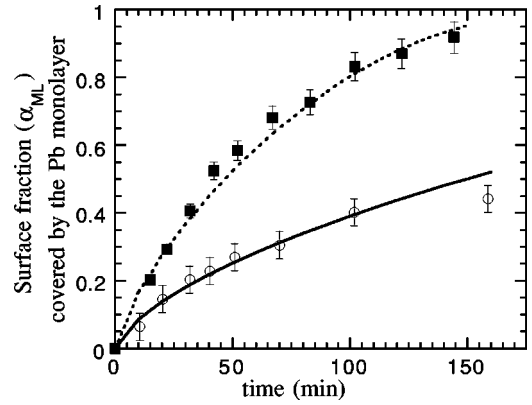
FIG. 8. Kinetics of reformation of the Pb monolayer with the $5\sqrt{2}$ structure between 3D Pb islands on a deposit achieved at RT and sputtered at 150 K. Symbols: AES results. Lines: adjustment by a simulation based on the numerical integration of a two-dimensional diffusion equation. Full squares: deposit preannealed at 530 K before sputtering; reformation temperature: 343 K. Open circles: unannealed deposit; reformation temperature: 250 K

represented in Fig. 8. The agreement in shape between measurements and simulation is remarkable. The simulation thus reproduces perfectly the two important features observed experimentally, which are (i) the fact, demonstrated by LEED, that the wetting layer reformation corresponds, since the be-
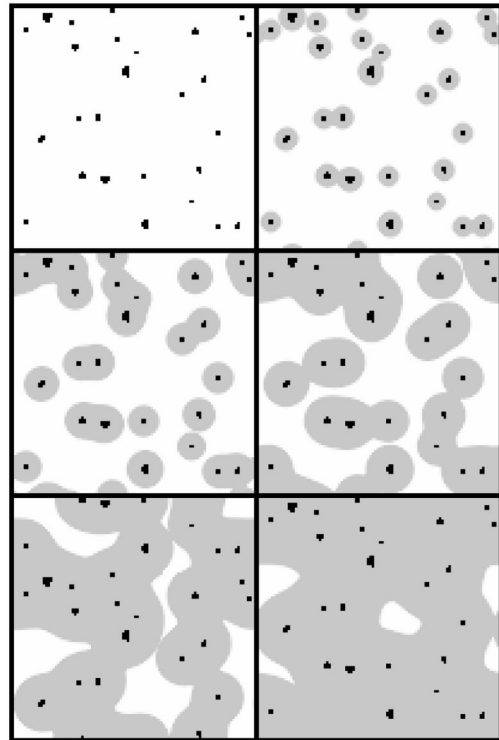
FIG. 9. Simulation of the reformation of the Pb wetting layer after sputtering at 150 K. The 3D Pb islands size and concentration result from deposit annealing at 530 K prior to sputtering. The top left panel exactly reproduces an image obtained by scanning electron microscopy. Reformation temperature: 343 K. The reformation state is represented in the figure for the following times (from top left to bottom right): 0, 10, 30, 60, 100, and 150 min. Image size: 40×40 μm^2.

ginning, to the growth of a $5\sqrt{2}$ structure with coverage θ_S; and (ii) the whole reformation kinetics measured by AES. To obtain this double agreement, we had to make the two following assumptions:

(1) As in the case of the higher-temperature domains studied in the preceding subsections, the diffusion of Pb atoms on the Cu substrate (i.e., for $\theta < \theta_S$) plays a minor role. It was not *a priori* obvious that this was still true in the lower-temperature range studied now, as the activation energies associated to diffusion above and below θ_S are different. However, our LEED observations do confirm this assumption. For the sake of simplicity, in the simulations we have set $D(\theta)=0$ for $\theta < \theta_S$.

(2) We have also assumed that the development of the wetting layer which forms around each 3D Pb island is isotropic. If it was markedly anisotropic, full coverage of the Cu substrate by the wetting layer would be hard to reach and, for high values of α_{ML}, the time evolution of $\alpha_{ML}(t)$ would be much slower than experimentally observed. In fact, setting, as we did in the 475–520 K temperature domain, $D_x \ll D_y$ cannot lead to simulated functions $\alpha_{ML}(t)$, properly adjusting the experimental kinetics. We were rather surprised by this fact as the LEED observations show that, in the wetting layer that reforms, one of the two $5\sqrt{2}$ structure types of domain is still favored. We thus have to admit (and we did not find any simple explanation for this fact) that the anisotropy in the domain distribution does not have the same consequences on the anisotropy of the wetting layer development at macroscopic and mesoscopic scales. The very good adjustment that is shown in Fig. 8 corresponds to $D_x = D_y$.

The fitting parameter leading to the adjustment of $\alpha_{ML}(t)$ in Fig. 8 is again the product $D_{ML}\epsilon$. In Fig. 10 we report, in an Arrhenius representation, two values of this product obtained from the fit of two functions $\alpha_{ML}(t)$ measured at reformation temperatures $T = 345$ K and 380 K, respectively. The striking fact, observed in Fig. 10, is that the corresponding points are perfectly aligned with the two points corresponding to the measurements of ''macroscopic'' deposit spread below T_M at 475 and 500 K (see Sec. V A 3). We thus confirm over five orders of magnitude (see Fig. 10) that the spread of the wetting Pb layer is very well represented by a single Arrhenius law. The associated energy is 0.97 ± 0.05 eV, and the associated preexponential factor is very high, corresponding to ''elementary jumps'' of a few thousand Å, as mentioned in Sec. V A 3.

In our experiments, we were able to check whether the Cu substrate surface was of high crystalline quality or perturbed by defects. Such a check could be achieved in a qualitative way by observing the width of the diffraction spots, in LEED patterns. A more quantitative information was provided by the measurement of the integral of the so-called ''surface peak,'' in RBS spectra recorded in channeling geometry.[29] We did perform such measurements to check the influence of sputtering at 150 K on the crystalline order of the substrate surface. We found that a significant disorder was produced, which was only removed by annealing above 500 K, i.e., above the temperatures at which we followed the reformation of the wetting layer. The analysis of the channeling data shows that this disorder corresponds to a rms static displacement, averaged over all the atoms of the 3–4 first atomic planes, of about 0.08 Å out of regular lattice sites. Such an
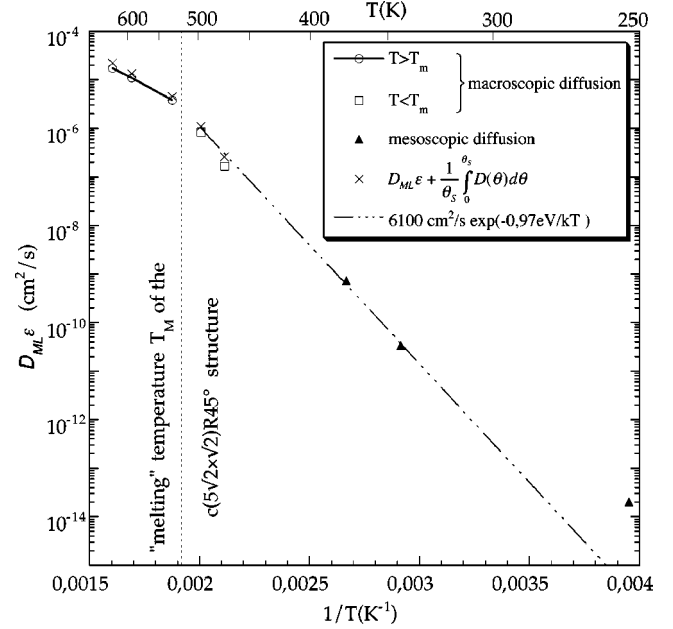
FIG. 10. Arrhenius representation of the temperature dependence of the product $D_{ML}\epsilon$ for all the experiments performed in this work. Circles: macroscopic RBS measurements above T_M; squares: macroscopic RBS measurements below T_M; triangles: mesoscopic Auger measurements. The triangle reported for the lowest temperature corresponds to wetting layer reformation from ''unannealed'' islands. The two other triangles correspond to wetting layer reformation from islands obtained after annealing at 530 K.

effect is probably due to interactions with extended defects, such as vacancy clusters, which were observed by STM after Cu sputtering.[30] However, the full consistency between the diffusion results obtained on the one hand at a macroscopic scale by RBS (on a surface preannealed at 800 K prior to Pb deposition) and, on the other hand, at a mesoscopic scale by AES, after sputtering at low temperature, indicates that this disorder does not affect significantly the reformation of the wetting layer. Thus the fact that a Pb adatom in its diffusion path has to cross some steps, associated with the existence of vacancy clusters, does not markedly modify the spreading velocity. This indicates that, even in presence of steps, the main diffusion barrier is still associated with domain boundary crossing.

2. Pb diffusion from ''unannealed'' Pb islands

We have also studied the kinetics of the wetting layer reformation on a deposit, which was not annealed at 530 K prior to sputtering at 150 K. The size of the 3D Pb islands is thus significantly smaller than in the case described in Sec.V B 1. We have used as a starting point for our simulation an image, performed *in situ* on such a deposit by STM,[2] which reveals that the island concentration is two orders of magnitude higher than in the image shown in Fig. 9; the mean distance between islands is 6000 Å instead of 6 μm. Our aim was to obtain the best possible adjustment of the function $\alpha_{ML}(t)$ extracted from AES measurements at a reformation temperature of 250 K. The simulations were performed as described in Sec. V B 1. The temporal behavior of the function $\alpha_{ML}(t)$ determined from the experiments was very different of the behavior observed in the case of Pb

islands previously annealed at 530 K. In particular, the reformation becomes abruptly extremely slow above $\alpha_{ML}=0.4$, which was not at all the case with ''annealed'' islands. In Fig. 8 we show a comparison between the function $\alpha_{ML}(t)$ determined from the analysis of the AES data and the simulation leading to the best fit up to $t=100$ min, which corresponds to $\alpha_{ML}=0.4$. The simulation can in no way predict the very slow variation of $\alpha_{ML}(t)$ observed for longer time.

The value of the product $D_{ML}\epsilon$ which corresponds to the fit shown in Fig. 8 is reported in Fig. 10. The corresponding point lies well above the extrapolation of the Arrhenius line, which fits the four other measurements performed below T_M by RBS or AES. This feature demonstrates that the reformation starts much faster than could be expected from all other measurements. The slowing observed when α_{ML} reaches 0.4 thus probably reflects the fact that, at this point, the product $D_{ML}\epsilon$ decreases toward a value closer to the extrapolation at 250 K of the Arrhenius line drawn in Fig. 10. We believe that this behavior is related to the formation of domain boundaries in the compact wetting layer, with $5\sqrt{2}$ structure, which grows around each island. Assume, as already conjectured, that the typical size of a domain is of the order of a few thousand Å. In the case of islands formed after preannealing at 530 K, this size is then at least one order of magnitude lower than the distance between the islands. In such a situation, numerous domain boundaries already exist for very low values of α_{ML}, and Pb diffusion on top of the wetting layer under reformation is limited by boundary crossing. Conversely, the mean distance between unannealed islands is of the same order of magnitude as the mean size of a domain. Thus, up to significantly high α_{ML}, the reformation of the wetting layer, on unannealed deposits, is not slowed down by domain boundaries.

The difference between preannealed and as-deposited Pb islands is of course not only their concentration, but also their size. One could then think that the adatom concentration ϵ in equilibrium with the unannealed islands, which are smaller, should be greater, leading to a higher value of the product $D_{ML}\epsilon$. However, the unannealed Pb islands already have lateral dimensions of few 1000 Å and a height of about 150 Å. The variation of ϵ when the size of the islands further increases is thus expected to be very small. Moreover, such an effect does not account for the slowing down of the wetting layer reformation above $\alpha_{ML}=0.4$.

VI. SUMMARY AND CONCLUSION

We have experimentally studied Pb diffusion in the Pb/Cu(100) system, above a saturation coverage θ_S. The

modeling and interpretation of the experimental results have been achieved in the simple frame of Fickian diffusion with diffusion coefficients depending on the Pb coverage θ. Such a description may of course be questioned when considering the strong inhomogeneities of the system studied, and the fact that, in some cases, we deal with diffusion at the scale of these inhomogeneities. However, this simple modeling allows us to satisfactorily describe all our experimental results.

We show that the main diffusion event, which leads to deposit spread, is the diffusion of Pb adatoms, on the top of the Pb wetting layer, in ''solid-gas'' equilibrium with 3D Pb islands. This diffusion event is much easier than Pb jumps on the Cu substrate. As a consequence, the spread leads to the growth of a compact wetting layer with a uniform coverage θ_S. Our results demonstrate that the structural state of the wetting layer affects the adatom diffusion in a decisive way. When this layer is ''melted,'' the length of elementary jumps of adatoms is of atomic size. In this case, the temperature dependence of the spread velocity arises both from the activation energy associated with these jumps and from the adatom formation energy E_S.

Below melting, the proportion of the two types of domains which form the $5\sqrt{2}$ structure of the wetting layer, and the mean size of individual domains at the scale of the diffusion lengths studied, both play a very important role. On top of a given domain, there is an easy direction for diffusion. Thus, if one domain orientation is markedly favored, a strong anisotropy of the deposit spread may take place. Moreover, the domain boundaries probably act as diffusion barriers. Then, when the diffusion lengths studied are greater than the mean domain size, the temperature dependence of the spreading velocity arises both from E_S and from the activation energy associated with domain boundary crossing. The corresponding slope in an Arrhenius representation is significantly steeper than when the wetting layer is melted (1 eV instead of 0.5 eV). In the same time the elementary jump length, deduced from the preexponential factor of the Arrhenius law, is found of about 1000 Å, which is the order of magnitude of domain size.

ACKNOWLEDGMENTS

[1] J. Henrion and G.E. Rhead, Surf. Sci. **29**, 20 (1972).

[2] F. Bocquet, Ph.D. thesis, University Paris VII, 1997; F. Bocquet, C. Cohen, J. Crestou, S. Gauthier, A. Rocher, and D. Schmaus, (unpublished).

[3] M. Zinke-Allmang, Thin Solid Films **346**, 1 (1999).

[4] B.K. Chakraverty, J. Phys. Chem. Solids **28**, 2401 (1967).

[5] J.A. Venables, G.D.T. Spiller, and M. Hanbücken, Rep. Prog.

Phys. **47**, 399 (1984).

[6] D. Beysens and C.M. Kobler, Phys. Rev. Lett. **57**, 1433 (1986).

[7] M. Zinke-Allmang, L.C. Feldman, and W. van Saarloos, Phys. Rev. Lett. **68**, 2358 (1992).

[8] J.A. Venables, Surf. Sci. **299-300**, 798 (1994).

[9] H. Brune, Surf. Sci. Rep. **31**, 121 (1998).

[10] M. Hanbücken, T. Doust, O. Osasona, G. Le Lay, and J.A. Ven-

ables, Surf. Sci. **168**, 133 (1986).

[11] N. Boutaoui, H. Roux, and M. Tholomier, Surf. Sci. **239**, 213 (1990).

[12] G. Raynerd, T.N. Doust, and J.A. Venables, Surf. Sci. **261**, 251 (1992).

[13] J.A. Venables, F.L. Metcalfe, and A. Sugawara, Surf. Sci. **371**, 420 (1997).

[14] H. Noro, R. Persaud, and J.A. Venables, Surf. Sci. **357-358**, 879 (1996).

[15] U. Kürpick, G. Meister, and A. Goldmann, Appl. Surf. Sci. **89**, 383 (1995).

[16] D.J. Chakrabarti and D.E. Laughlin, Bull. Alloy Phase Diagrams **5**, 503 (1984).

[17] W. Hösler and W. Moritz, Surf. Sci. **175**, 63 (1986).

[18] C. Cohen, Y. Girard, P. Leroux-Hugon, A. L'Hoir, J. Moulin, and D. Schmaus, Europhys. Lett. **24**, 767 (1993).

[19] C. Nagl, E. Platzgummer, O. Haller, M. Schmid, and P. Varga, Surf. Sci. **331-333**, 831 (1995).

[20] S. Robert, S. Gauthier, F. Bocquet, S. Rousset, J.-L. Duvault, and J. Klein, Surf. Sci. **350**, 136 (1996).

[21] E. Platzgummer, M. Borrell, C. Nagl, M. Schmid, and P. Varga Surf. Sci. **412-413**, 202 (1998).

[22] J.P. Bibérian and M. Huber, Surf. Sci. **55**, 259 (1976).

[23] A. Sánchez and S. Ferrer, Phys. Rev. B **39**, 5778 (1989).

[24] S. Robert, Ph.D. thesis, University Paris VII, 1995.

[25] G. Rao, D.B. Zhang, and P. Wynblatt, Acta Metall. Mater. **41**, 3331 (1993).

[26] F. Abel, C. Cohen, J.A. Davies, J. Moulin, and D. Schmaus, Appl. Surf. Sci. **44**, 17 (1990).

[27] C. Cohen, J.A. Davies A.V. Drigo, and T.E. Jackman, Nucl. Instrum. Methods **218**, 147 (1983).

[28] J. Crank, in *The Mathematics of Diffusion* (Oxford University Press, New York, 1975).

[29] I. Stensgaard, L.C. Feldman, and J.P. Silverman, Surf. Sci. **77**, 513 (1978).

[30] J.C. Girard, Y. Samson, S. Gauthier, S. Rousset, and J. Klein, Surf. Sci. **302**, 73 (1994).